
Evaluation of an LES Code Against a Hydrogen Dispersion Experiment

Nektarios Koutsourakis^{1,2,*}, Ilias C. Toliás¹, Alexander G. Venetsanos¹ and John G. Bartzis²

¹ Environmental Research Laboratory, NCSR Demokritos
15310 – Aghia Paraskevi, GREECE

² Environmental Technology Laboratory, Department of Mechanical Engineering
University of West Macedonia, 50100 – Kozani, GREECE

Received: 03/07/2012 – Revised 05/08/2012 – Accepted 26/11/2012

Abstract

The Large Eddy Simulation (LES) methodology is used nowadays not only as a research tool, but also for practical applications. Given this fact, an LES code which specializes in turbulent dispersion problems has been developed. It has been incorporated into the well established in atmospheric and hydrogen dispersion applications ADREA-HF Computational Fluid Dynamics (CFD) code. In this study, the LES methodology is evaluated against a hydrogen release and dispersion experiment in a hallway that has ventilation openings. Results from Reynolds Averaged Navier Stokes (RANS) methodology and from the Fire Dynamics Simulator (FDS) LES code are also included. The hydrogen concentration values predicted with ADREA-HF LES are very close to the measured ones, especially for the sensors close to the ceiling. The study includes comments about critical parameters used in the LES models, like the value of the Smagorinsky constant. Finally several advantages of the LES methodology are outlined.

Keywords: Large Eddy Simulation, LES, dispersion, hydrogen, ADREA-HF

1. Introduction

1.1. Background

While the CFD methodology was first used more than 100 years ago [1], the foundations of Large Eddy Simulation has less than half of a century of age [2-6]. Initially, the research team of National Center for Atmospheric Research at Colorado and later on the scientists of Stanford University were the pioneers of the Large Eddy Simulation development. Originally used mainly for turbulence research, this methodology resolves the large, energy containing eddies in a time-dependent manner, being able to accurately capture the flow field in cases where time-averaged methodologies like RANS may fail, as for example in unsteady or recirculating flows. On the other hand, the computational cost is in some cases prohibitive, since in order to well-resolve the near-wall region the simulation time is proportional to $Re^{2.4}$ [7], where Re is the Reynolds number. That is the main reason why LES was not considered for

* Corresponding Author: N. Koutsourakis

Email: nk@ipta.demokritos.gr Telephone: +0030 2106503408

© 2013 All rights reserved. ISSR Journals

Fax: +0030 2106525004

PII: S2180-1363(12)4225-X

practical applications more than a decade ago. However, the use of wall functions along with the low-cost computational power increase has nowadays changed that. Since the physical phenomena involved in atmospheric dispersion applications usually have an unsteady character, the LES emerges as a promising technique to cope with those problems. The recently developed ADREA-HF LES has already been tested in flow and dispersion problems [8, 9, 10]. As part of the validation procedure of the code, it was considered necessary to evaluate it against a more difficult dispersion case, involving a buoyant gas in a non-trivial geometry.

1.2. Description of the experiment and previous simulation studies

Hydrogen special characteristics as an energy carrier have attracted the research interest in recent years [11]. One of the main problems that should be addressed is the safety, since hydrogen has a wide flammability limit (4-74 % v/v) that makes its storage and handling hazardous [12]. Several experiments in (partly) confined spaces have been conducted in the past [13-16] in order to evaluate possible risks from hydrogen leakages.

The particular experiment examined here represents a half-size hallway with dimensions 2.9 m × 0.74 m × 1.22 m (length, width, height) [13]. Hydrogen leaks from the floor at the left end of the hallway, Figure 1, for a period of 1200 s. At the right end there are a roof vent and a lower door vent for natural ventilation. The hydrogen flow rate is $9.43833 \times 10^{-4} \text{ m}^3/\text{s}$. Four sensors were used to record the local hydrogen volumetric concentration with time. Table 1 shows the various geometrical characteristics. For the given volumetric flow rate and leak area the hydrogen exit velocity is 0.02032 m/s with a volume concentration equal to 1.0 at the leak.

Several CFD simulation studies exist for this experiment. Swain et al. [13] performed a RANS study using the Fluent code and found very good agreement with the measurements. He first calibrated the CFD model to agree with the experimental helium data and then used it to predict the hydrogen concentration distribution. Later Agranat et al. [17] used the PHOENICS code with a grid of 6480 cells and found an overprediction for sensors 2 and 3. The concentration isosurfaces near the ceiling had very similar shape to those of Swain et al. [13] though. Matsuura et al. [18] used the CFD ACE+ code with various grids. The results presented had some disagreements compared to the experiment, especially at sensor 4. Parametric analysis performed with the 28500 cells' grid for different physical and geometrical parameters provided possible explanations for the discrepancies observed. The first LES study of this experiment, using the FDS code, was performed recently from Matsuura [19] and Matsuura et al. [20], who found good agreement against the experimental data with their dense grid of 290000 cells, especially at the sensors close to the ceiling. Except of this experiment, the LES methodology has being used for various hydrogen release applications during the last years [21-25].

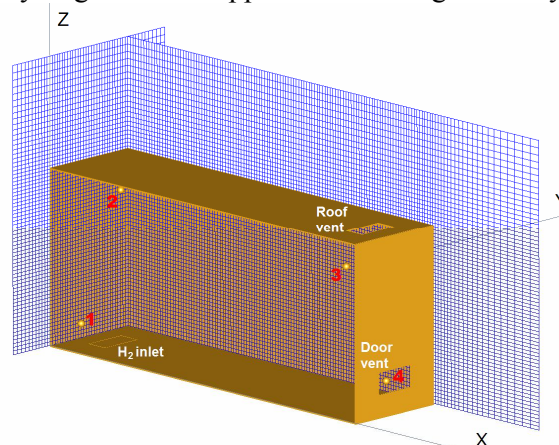


Figure 1. The hallway, sensors 1-4, hydrogen inlet, door and roof vents and two planes of the finer computational mesh. Front hallway wall is hidden

TABLE I: GEOMETRICAL CHARACTERISTICS

	X (m)	Y (m)	Z (m)
Hallway size	2.90	0.74	1.22
Sensor 1 location	0.1524	0.144	0.1524
Sensor 2 location	0.1524	0.5208	1.0088
Sensor 3 location	2.6762	0.144	1.0088
Sensor 4 location	2.6762	0.5208	0.1524
Roof vent size	0.1524	0.3048	0.00
Roof vent location	2.6	0.2176	1.22
Door vent size	0.0	0.3048	0.1524
Door vent location	2.9	0.2176	0.1524
H ₂ inlet size (leak)	0.1524	0.3048	0.00
H ₂ inlet location (leak)	0.1524	0.2176	0.00

2. Numerical procedure

2.1. Governing equations

In LES, a spatial filtering is applied to every variable of the flow field, decomposing it into a resolved (or filtered) component and an SGS component. The filtered governing equations are:

$$\frac{\partial \bar{p}}{\partial t} + \frac{\partial (\bar{\rho} \tilde{u}_i)}{\partial x_i} = 0 \quad (1)$$

$$\frac{\partial (\bar{\rho} \tilde{u}_i)}{\partial t} + \frac{\partial (\bar{\rho} \tilde{u}_i \tilde{u}_j)}{\partial x_j} = - \frac{\partial \bar{p}}{\partial x_i} + \frac{\partial (\tilde{\tau}_{ij}^l + \tau_{ij}^R)}{\partial x_j} \quad (2)$$

$$\tilde{\tau}_{ij}^l + \frac{2}{3} \mu \frac{\partial \tilde{u}_k}{\partial x_k} \delta_{ij} = 2 \mu \tilde{S}_{ij} \quad (3)$$

$$\tilde{S}_{ij} = \frac{1}{2} \left(\frac{\partial \tilde{u}_i}{\partial x_j} + \frac{\partial \tilde{u}_j}{\partial x_i} \right) \quad (4)$$

$$\bar{p} = \bar{\rho} r \bar{T}, \quad (5)$$

where ρ is the density, t is the time, u_i are the velocity components, x_i is the distance, p is the pressure, τ_{ij} are the stress tensor components, μ is the kinematic viscosity, δ_{ij} is the Kronecker delta, S_{ij} is the rate-of-strain tensor, r is the gas constant, T is the absolute temperature. The bar ($\bar{\quad}$) represents space-averaged instantaneous values, while the tilde ($\tilde{\quad}$) denotes density-weighted Favre-averaging. $\tilde{\tau}_{ij}^l$ is the instantaneous shear stress tensor due to molecular forcing and τ_{ij}^R is the residual stress tensor due to the subgrid turbulence, modelled using the classical Smagorinsky subgrid scale model, as:

$$\tau_{ij}^R + \frac{1}{3} \tau_{kk} \delta_{ij} = 2 \mu_t \tilde{S}_{ij} \quad (6)$$

$$\mu_t = \bar{\rho} \left[C_s \Delta \left(1 - e^{-y^+/25} \right) \right]^2 \sqrt{2 \tilde{S}_{ij} \tilde{S}_{ij}}, \quad (7)$$

where y^+ is the non-dimensional distance from the wall. The Smagorinsky constant C_s has a default value of 0.1. The term $\frac{1}{3} \tau_{kk} \delta_{ij}$, which is usually negligible compared to thermodynamic pressure [26], is incorporated into the filtered pressure. The filter-related Δ is taken as $\Delta = V^{1/3}$, where V is the volume of the computational cell. In equation (7), the Van-Driest damping [27] is incorporated, in order to account for the reduced growth of the small scales near the wall.

The filtered scalar mass transport equation for a passive component i of a mixture, is:

$$\frac{\partial(\bar{\rho}\tilde{q}_i)}{\partial t} + \frac{\partial(\bar{\rho}\tilde{u}_j\tilde{q}_i)}{\partial x_j} = \frac{\partial}{\partial x_j} \left(\left(\bar{\rho}D_i + \frac{\mu_{sgs}}{Sc_{sgs}} \right) \frac{\partial\tilde{q}_i}{\partial x_j} \right), \quad (8)$$

where q_i is the mass fraction of the component i , D_i is the molecular diffusivity of the component i (molecular diffusivity of hydrogen in air is equal to $7,8 \times 10^{-5} \text{ m}^2/\text{s}$), μ_{sgs} is the subgrid-scale kinematic viscosity and Sc_{sgs} is the turbulent subgrid scale Schmidt number, taken equal to 0.72. In this equation the modelling of the subgrid-scale scalar stress via an eddy gradient diffusion hypothesis is incorporated.

2.2. The numerical tool

ADREA-HF uses the finite volume method on a staggered Cartesian grid. The geometry is reproduced with the use of porosities, which makes possible the correct representation of any solid surface on a structured mesh [28]. The pressure and velocity equations are decoupled with the use of the ADREA/SIMPLER algorithm [29]. For the discretization of the convective terms a second order accurate deferred correction central scheme [30] was used. For the time advancement, a second order accurate Crank-Nicolson numerical scheme was chosen. The time step is automatically adapted according to prescribed error bands and desired Courant–Friedrichs–Lewy (CFL) number. For the concentration calculation, a second order accurate linear upwind scheme was used, along with a SMART limiter in order to increase the numerical stability. ADREA-HF is parallelized in both shared memory architectures with the use of OpenMP directives and in distributed memory architectures, using MPI. For the current runs, the Krylov subspace method BiCGstab is used, with the additive Schwarz preconditioner [31]. Both the creation of the preconditioner and the solution of the preconditioner system are done in parallel.

2.3. The simulation approach

LES simulations with ADREA-HF. The whole room with its openings is simulated and its geometry reproduced. Following the experience of another similar study [32], the computational domain is extended outside the building for 1.01 m in the x direction, for 0.78 m at the z direction and for 0.35 m at each side of the building at the y direction (blocked cells till $x = 2.9$ m and till $z = 1.22$ m). A sensitivity test, that was performed for the expansion of the domain and for the blocked cells, revealed that the above-mentioned choices are suitable for the correct reproduction of the experiment. Several grids are tested in order to assess the sensitivity of the results on the cell size. The basic grid has $93 \times 37 \times 47$ cells in the x , y and z directions respectively (122815 non-blocked cells), while inside the hallway the cell is about 0.038 m. A typical run time for this grid using 4 processing cores of a modern personal computer is about four days. Runs with two coarser grids with 16736 and 40176 cells and two finer grids with 214122 and 373632 cells are also performed. Figure 1 presents the finer grid with $137 \times 52 \times 70$ cells and with a typical cell size of about 0.025 m. All grids are aligned with the area source and with the exits, since this meshing provided better results. In all exit planes (lateral, front, back and top) the non-reflecting boundary conditions for the normal velocities are chosen, while for the parallel to the exit planes' velocity components, Neumann boundary conditions are applied. Zero gradient is also utilized for the mass fraction of hydrogen, with the additional restriction that no hydrogen enters the flow field from those planes in the case of inflow. The source is modeled as a jet surface with given values of mass and momentum. Pure hydrogen with no diffusion is emitted, in order to assure the desired fluxes. All solids are impermeable to both hydrogen and air. The default rough-type wall functions are used with a roughness length of $z_0=0.001$ m. Sensitivity tests performed firstly with other roughness length and secondly with smooth type of wall functions did not reveal any large changes, especially for the sensors close

to the ceiling. In the simulations, the values of the non-dimensional distance from the wall y^+ are from 0 to 100. As initial conditions, a stagnant flow field with no turbulence and no hydrogen is specified, along with a given temperature of 288.15 K. No energy equation is solved. The hydrogen is treated as an ideal gas with viscosity 8.8×10^{-6} kg/m/s. The reference pressure is 101325 Pa. The time step is set automatically by the code with a restriction of maximum CFL number in each cell equal to 0.6. Consequently, the average time step for the dense grid is about 0.015 s which is much smaller than the typical turbulent time scales of the flow as estimated by RANS simulation. Runs with different time steps were also performed and time step independency was confirmed.

LES simulations with FDS. This particular LES code is chosen for comparison since it is extensively validated [33] and is already tested against hydrogen release cases [19-20, 25, 34]. The general simulation approach, the geometry and the grids are the same with those of ADREA. The numerical options are left at their default values, except for the Smagorinsky constant, for which the value of $C_s = 0.1$ is chosen, since results with the default $C_s = 0.2$ had severe discrepancies compared to the experimental values. That is also in agreement with previous hydrogen dispersion studies [10,34], where the Smagorinsky constant $C_s = 0.1$ had provided much better results compared to $C_s = 0.2$. The description of the code can be found at the FDS Technical Reference Guide [35].

RANS simulations with ADREA-HF. The RANS version of ADREA-HF is selected for comparison since it is also extensively used in hydrogen applications [28]. The default $k-\epsilon$ model is applied as the turbulence closure scheme and the turbulent Schmidt number is 0.72. In order to assess the grid independency, the results from five different grids (of 15540, 39684, 104440, 185376 and 318768 cells) are investigated. The time step independency of the runs was also assured.

3. Results and discussion

3.1. General presentation of the results and of the dominating physical phenomena

Figure 2 shows the propagation of the plume with time. First a hydrogen column is formed, that goes towards the ceiling. Then the hydrogen accumulates at the ceiling for some dozens of seconds, until the roof vent is reached and after that part of the hydrogen starts escaping from the room. Fresh air is entering from the door vent and a flow circulation along the whole room takes place, as can be seen at Figure 3.

In Figure 3, the stratification of hydrogen after reaching a more or less statistically stable state is presented. At the upper half of the room the concentration level is above 4% and the concentration gradients are low. The buoyancy of hydrogen causes the circulation of the flow in the room. The air entering from the door vent heads towards the floor due to its higher density, travels along the floor until it reaches the leakage area and shifts the hydrogen updraft towards the left wall. The strong updraft drives the flow, which continues along the ceiling till the roof vent. Near the left wall plane, smaller recirculations (A1, A2 at Figure 3) are formed.

3.2. Evaluation of CFD against experimental results

In Figure 4 the concentration values from the CFD results are evaluated quantitatively against the experimental measurements. In general, CFD predictions (especially those of ADREA-HF LES) are quite good, given the difficulty of calculating the flow of a buoyant mixture and given the fact that sensors 1 and 4 are placed at tricky points. All presented CFD results are with the densest grids and can be considered as grid-independent. Of course RANS cannot capture the variations of the instantaneous values like LES. That is one of the major advantages of LES in the specific case of hydrogen release and more generally in dispersion studies. For instance, at sensor 1 RANS simulation predicts hydrogen concentration one order of

magnitude below the flammability limit, while the LES simulations reveal many times higher instantaneous values, which are very often above the limit of 1%, which is considered as a safety margin [16].

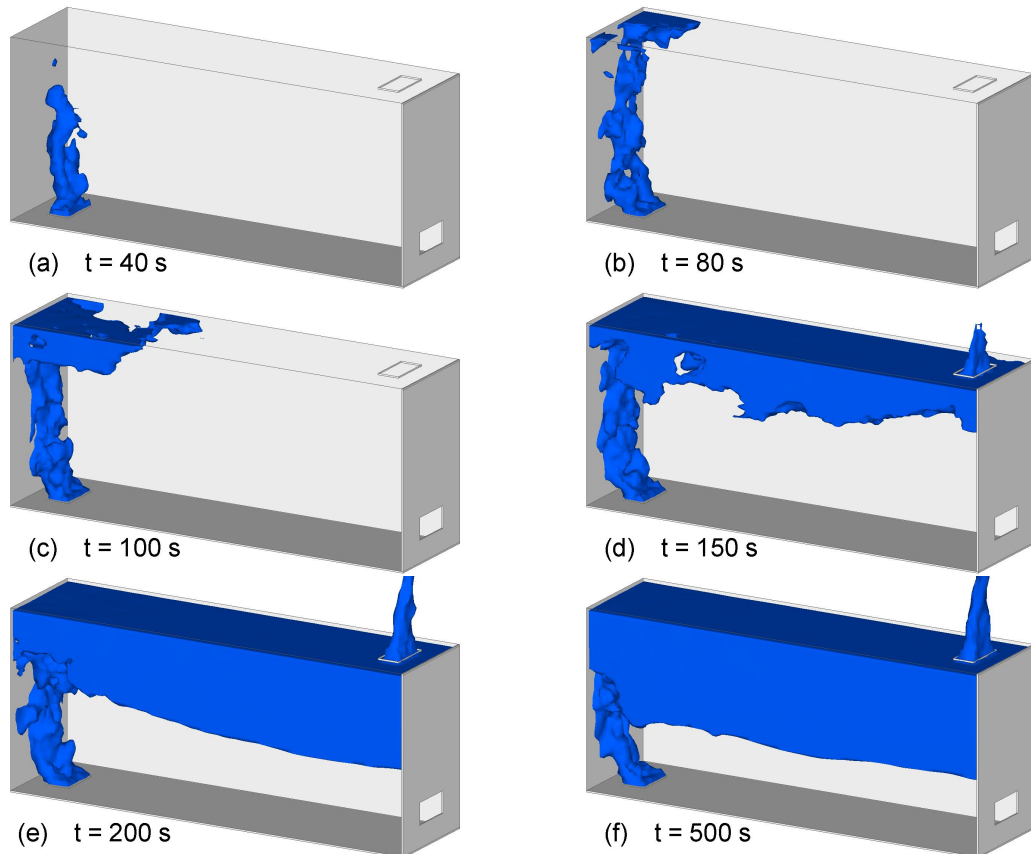


Figure 2. Hydrogen isosurfaces of 4% vol. at different times of the experiment. The front and the top walls of the hallway are removed

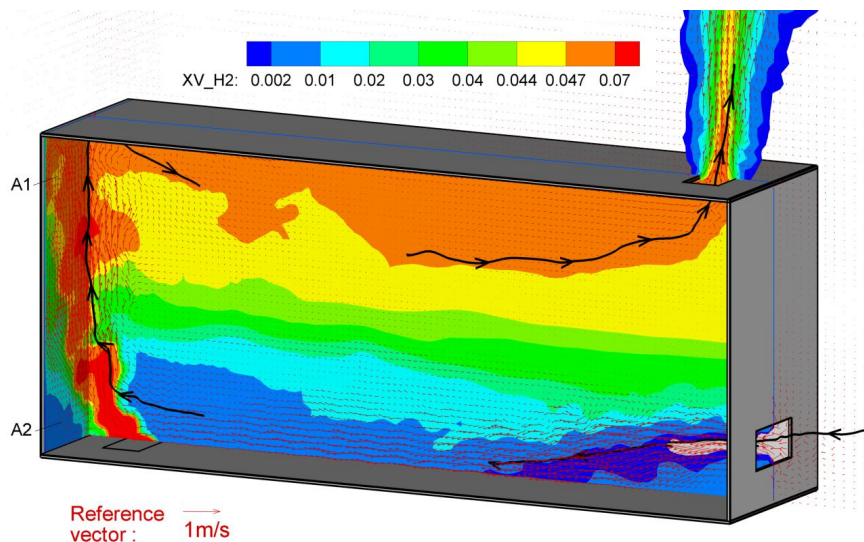


Figure 3. Hydrogen concentration contours at two planes (plane A: $X=0.02$ m, plane B: $Y=0.37$ m), 800s after the beginning of the release. The instantaneous tangential velocity vectors and three characteristic short stream traces (in 3-D) can also be seen. A1, A2 denote recirculation regions

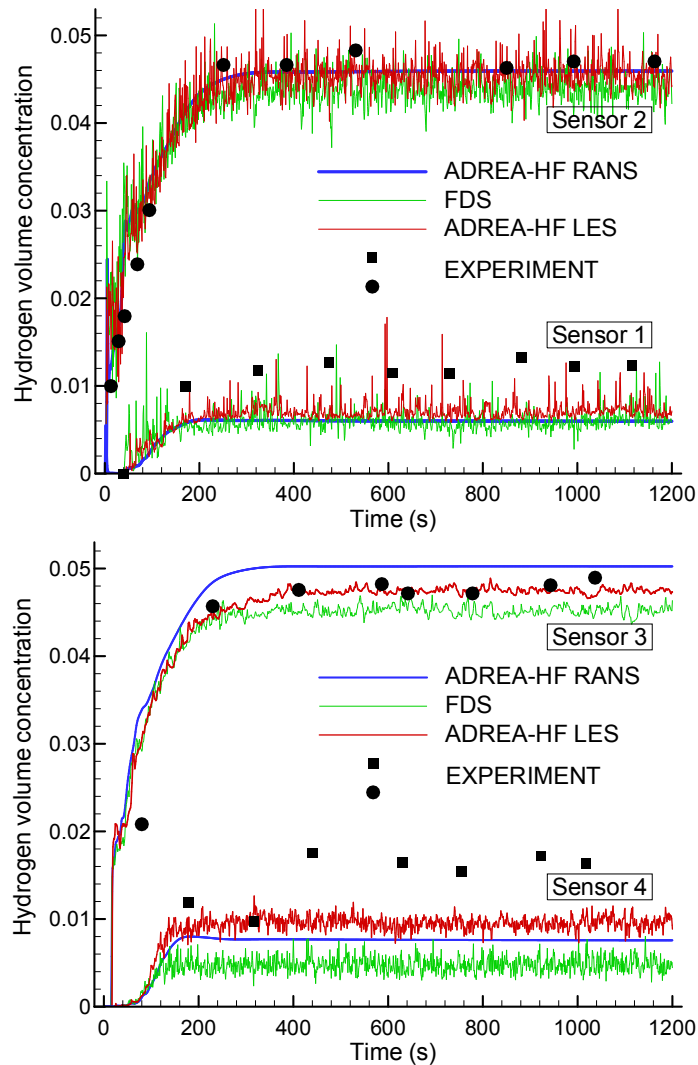


Figure 4. Comparison of the ADREA-HF LES calculated concentration time series with the experimental values at each sensor. Results with the ADREA-HF RANS and with the FDS code with $C_s = 0.1$ are also included. In all cases the densest grids are used

From the LES runs it is observed that sensor 1 presents the highest turbulent variations and peaks due to its proximity to the source, while sensor 3 presents the lowest, since it is in an area where the flow is more settled. At sensor 4 the variability of concentration values increases partly due to its proximity to the door vent, from where the air enters the room and disturbs the flow field. Tests performed with FDS and medium grids, revealed that with $C_s = 0.2$, the concentration values were significantly lower, especially for sensors 1 and 4 (about 50% lower). The variations were also lower. The low concentration variations of simulations with $C_s = 0.2$ can also be observed at previous hydrogen dispersion studies [10,19,34]. That is due to the fact that the turbulent dissipation with $C_s = 0.2$ is too high to let the resolved turbulence develop. Thus the value of $C_s = 0.2$ should be avoided and the value of $C_s = 0.1$ is preferred for hydrogen dispersion studies.

Sensor 1, which is above the west (left) end of the leaking area and close to the south (front) wall, is in an area of high concentration gradients. The concentration increases towards the north-west side of the sensor. That happens because the core of the leaking hydrogen is transferred towards the west wall due to the developed flow field. Therefore, at short distance

above the source area the hydrogen concentration drops quickly (Figure 3). That might be a possible explanation for the difficulty to accurately predict the hydrogen concentration of sensor 1. Another reason could be the complex turbulent mixing of the door-vent draft with the buoyant updraft of hydrogen above the source [18]. The underestimation at the particular sensor could also be explained from the supposed turbulence of the entering hydrogen, which was not documented. That would result in higher turbulent dispersion close to the inlet and consequently higher concentration values at positions outside the core of the plume. Furthermore, the experimental uncertainties for the particular sensor are very high: in a duplication of the experiment from Inoue, presented from Matsuura et al. [18], the concentration values at sensor 1 were significantly lower than those of the original experiment of Swain and much closer to the current CFD results.

The CFD volume fraction concentration values for the ceiling's sensors 2 and 3 are very close to the experimental ones, especially for the ADREA-HF LES code. Indeed, the values at those sensors are mainly influenced from the amount of hydrogen that enters the room and from the hydrogen density, which are accurately known. After a statistically steady state is reached, the amount of hydrogen that enters the room is equal to that leaving the room. Since the concentration gradients close to the roof are small, predictions there are easier to perform.

Sensor 4 is far away from the source and it is close to the door vent, which adds more uncertainties to the modeling. It is also in a region of high concentration gradients. For that reason the predictions of all models at that sensor are worst compared to the predictions at the other sensors. One possible explanation for the underestimation at sensor 4, is that in the experiment the fresh air entering the room did not deviate towards the floor as predicted in the simulation (Figure 3), i.e. the air in the experiment either entered with higher velocity and with a direction parallel to the floor, or, more probably, entered with very low velocity and deviated immediately towards the floor, with a very high angle. Either way sensor 4 would be outside the mainstream of the fresh air (Figure 3) and thus would provide higher concentrations. Indeed, a parametric study performed from Matsuura et al. [18] reveals that a minor pressure difference between the door vent and the roof vent would result in significant differences of the flow field inside the room. For this or other reasons, like a possibly unequal heating of the room walls, the experiment might not be perfectly reproduced from CFD and that could explain the discrepancies at sensor 4. The difficulties of the particular experiment and the severe dependence of its results on various undocumented physical parameters can also be understood from the fact that in the duplication of the experiment from Inoue, the concentration values were different at all the sensors. Particularly at sensor 4, the experiment of Inoue provided lower concentrations, very close to those predicted from ADREA-HF simulations.

Another possible explanation for the discrepancies is the fact that the sensors are not on the *central* constant- y plane of the room. The coordinations of the sensors at y axis are different: Sensors 1 and 3 are in front of the front side of the openings/source (Figure 1), while sensors 2 and 4 are aligned with the back side of the openings. This means that the measurements were vulnerable to any asymmetries that might occur, especially for sensor 4, which is close to the air intake and could be influenced even from asymmetric physical conditions outside the room, as those mentioned previously. The underprediction at sensor 4 can also be found in other studies of this experiment [17-19]. In order to be able to assess any possible experimental asymmetries, it is suggested for future experiments to have additional measurements at symmetric points, with symmetry plane the central constant- y plane of the room.

It can be seen that the ADREA-HF RANS and LES results are closer with each other (and with FDS results) than with the experimental data, due to the common grounds of the CFD methodology. Of course, RANS is expected to provide less accurate results at places where the turbulent flow is more complex and highly unsteady. This might be an explanation of the superior performance of ADREA-HF LES close to the source (sensor 1) and close to the door vent (sensor 4). Another advantage of LES is that it can provide detailed Reynolds stresses and

more generally higher-order moments of the resolved variables. Finally, LES is an inherently time-dependent methodology and is more suitable for such problems, while RANS is mainly targeting to steady-state cases. On the other hand, LES is much more demanding in computational resources. Current RANS simulations were several times faster compared to the corresponding LES simulations.

Concerning the two LES codes, ADREA-HF and FDS, they behave similarly regarding the concentration fluctuations. In the average values though, ADREA-HF is closer to the experiment. This is not attributed to the different default turbulent Schmidt number used by the two codes ($Sc_{sgs} = 0.72$ for ADREA-HF and $Sc_{sgs} = 0.5$ for FDS), since sensitivity tests with different Schmidt numbers reveal no severe impact on the results. Indeed, in LES the turbulent Schmidt number only affects the subgrid scale and its influence on the final concentration values is not crucial, especially if dense grids are used. It should be reminded that FDS results in Figure 4 are with $C_s = 0.1$. The FDS results with the default value of C_s equal to 0.2, are much worst, with very low variations.

3.3. Grid independency and further comments on all runs performed

At Figure 5, for each code used, the results for all grids are presented in order to assess the grid independency. For this figure, the average values between 400 s and 1200 s are considered; this interval represents the “steady state” part of the experiment. The experimental values are also added to the diagrams. All LES results are with $C_s = 0.1$.

It should be noted that in RANS and LES the grid independency does not have exactly the same meaning. In LES, as the grids are getting finer, more and more turbulent structures are resolved and the solution tends to the direct numerical simulation (DNS) solution. In coarser grids, the Smagorinsky constant C_s should be higher in order to compensate for the non-resolved turbulence. On the other hand, the denser the grid, the less important the C_s value is.

It is clear, especially for the ADREA-HF simulations, that the results tend to a specific, grid-independent solution. At the ceiling sensors, the grid independent solution of ADREA-HF LES is less than few per cent different compared to the experiment. RANS overpredicts at sensor 3, while FDS underpredicts at both ceiling sensors.

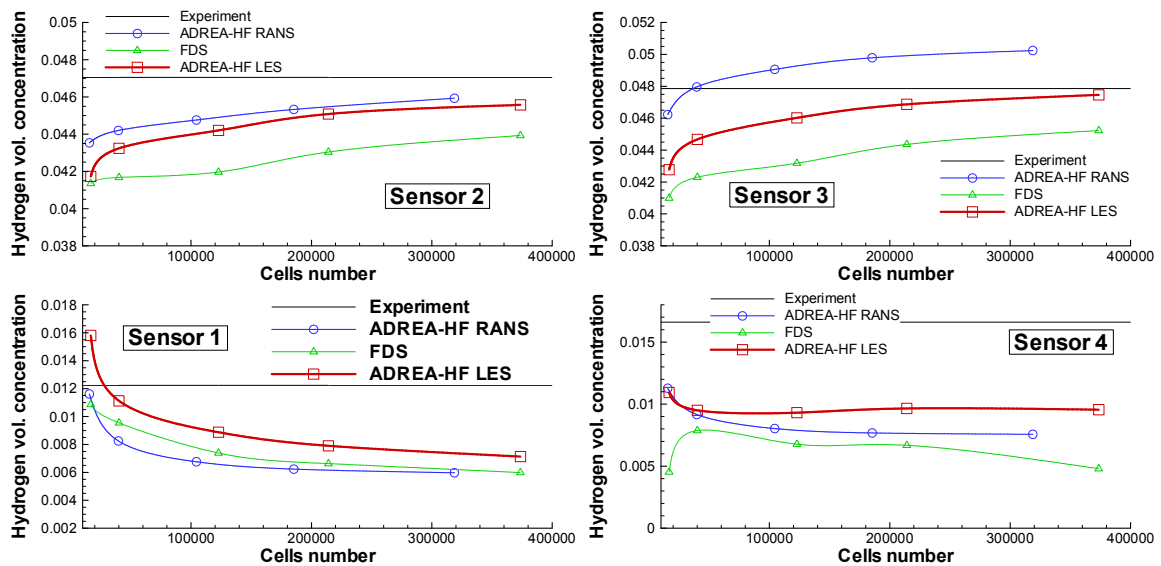


Figure 5. Concentration values (averages between 400 s and 1200 s) for all sensors for all simulations performed, in order to assess the grid independency

At the bottom sensors, where the concentration values are significantly lower, all codes underpredict and that was thoroughly discussed in the previous sub-section. ADREA-HF LES presents the better performance. At sensor 1 that is closer to the source, the grid independency is more difficult to achieve, as commented in a previous study [10]. For FDS the grid independency curves are not that smooth, especially for sensor 4. That could be an indication of the strong unsteady characteristics at the neighborhood of that sensor and of the uncertainties of the results. The LES study of Matsuura et al. [19] had also discrepancies compared to the experiment at the bottom sensors. It is reminded however that the experiment has also very high uncertainties for those sensors, which are placed at positions of high concentration gradients.

At sensors 2 and 3 the predicted concentrations are of the same order of magnitude (“high”). Similarly, the predictions at the sensors 1 and 4 give “low” concentrations. It should be commented that the ratio of “high” (at sensors 2, 3) to “low” (at sensors 1, 4) concentrations (or the difference of “high” minus “low” concentration) is overpredicted in all CFD simulations of this work, but also in almost all the CFD studies of this particular experiment [17-20].

At sensor 1, the coarser grids provide predictions closer to the experimental values. This is a good example of the need to perform grid independency studies. The finer grids’ simulations, with less numerical diffusion and better representation of the flow field (like the more accurate reproduction of the corner recirculations A1 and A2 in Figure 3) reveal that in the specific case, the “good” performance of CFD with coarse grids is misleading.

Summing up, it is clear from Figures 4 and 5 that ADREA-HF LES provides the best overall performance.

4. Conclusions

The LES methodology, which is recently incorporated into the ADREA-HF code, performs very well in this difficult-to-predict experiment. The calculated concentration variations are very similar to those of FDS, which is a validated LES code that has been applied to hydrogen applications in the past. Actually, the predictions of the current LES methodology are closer to the experimental values than those of FDS. Along with a similarly good performance of ADREA-HF LES in another hydrogen release experiment [10], this particular methodology can be trusted as a reliable tool for dispersion studies and help in decision support, design procedures and hydrogen safety assessment.

Another conclusion is the fact that in some occasions coarse grids can deceptively provide better results. Therefore, the researcher should perform a grid independency study, in order not to be misled.

Concerning the Smagorinsky constant, it is confirmed that the $C_s = 0.1$ value is to be preferred to the (too dissipative) $C_s = 0.2$ value for hydrogen dispersion studies.

Concerning LES and RANS comparison, it is shown that LES can capture the time-dependency of the phenomenon, it can provide minimum and maximum values of instantaneous concentrations and it can be more accurate in complex parts of the flow. On the other hand it is several times slower than RANS.

Acknowledgements

This work was partly supported from the State Scholarships Foundation and from the Municipality of Aghia Varvara Attikis, Greece. The authors would like to thank Miss S. G. Giannissi for critical reading of the manuscript.

References

- [1] L.F. Richardson, *The approximate arithmetical solution by finite differences of physical problems involving differential equations, with an application to the stresses in a masonry dam*. Philosophical Transactions of the Royal Society, 1911. **A 210**: p. 307-357.
- [2] J. Smagorinsky, *General circulation experiments with primitive equations*. Monthly Weather Review, 1963. **93**(3): p. 99-164.
- [3] D. K. Lilly, *The representation of small-scale turbulence in numerical simulation experiments*. in *Proceedings of the IBM scientific computing symposium on environmental sciences*. 1967. Yorktown Heights, N.Y. p. 195.
- [4] J. W. Deardorff, *A numerical study of three-dimensional turbulent channel flow at large Reynolds numbers*. Journal of Fluid Mechanics, 1970. **41**: p. 453-480.
- [5] A. Leonard, *Energy cascade in large eddy simulation of turbulent fluid flows*. Advances in Geophysics, 1974. **18A**: p. 237-248
- [6] U. Schumann, *Subgrid scale model for finite difference simulations of turbulent flows in plane channels and annuli*. Journal of Computational Physics, 1975. **18**: p. 376-404.
- [7] U. Piomelli. *Large-eddy and direct simulation of turbulent flows*. in *CFD2001 - 9e conférence annuelle de la Société canadienne de CFD*. 2001. Kitchener, Ontario. <http://terpconnect.umd.edu/~ugo/research/figs/CFD01.ps.gz> (accessed 3-7-2012).
- [8] Koutsourakis, N., Venetsanos, A.G., Bartzis J.G. and I.C. Tolias. *Presentation of new LES capability of ADREA-HF CFD code*. in *Proceedings of the 13th International Conference on Harmonisation within Atmospheric Dispersion Modelling for Regulatory Purposes*. 2010. Paris, France. p. 662-666.
- [9] Koutsourakis, N., Venetsanos, A.G., Bartzis, J.G., Tolias, I.C. and N.C. Markatos. *Pollutant dispersion study in asymmetric street canyons using Large Eddy Simulation*. in *7th GRACM International Congress on Computational Mechanics*. 2011. Athens, Greece.
- [10] Koutsourakis, N., Venetsanos, A.G and J.G. Bartzis, *LES modelling of hydrogen release and accumulation within a non-ventilated ambient pressure garage using the ADREA-HF CFD code*, International Journal of Hydrogen Energy, 2012. **37**: p. 17426-17435.
- [11] Nowotny, J. and T.N. Veziroglu, *Impact of hydrogen on the environment*. International Journal of Hydrogen Energy, 2011. **36**: p. 13218-13224.
- [12] Rigas, F. and S. Sklavounos, *Evaluation of hazards associated with hydrogen storage facilities*. International Journal of Hydrogen Energy, 2005. **30**(13-14): p. 1501-1510.
- [13] Swain, M.R., Grilliot, E.S. and M.N. Swain, *Experimental verification of a hydrogen risk assessment method*. Chemical Health & Safety, 1999. **6**(3): p. 28-32.
- [14] Gupta, S., Brinster, J., Studer, E. and I. Tkatschenko, *Hydrogen related risks within a private garage: concentration measurements in a realistic full-scale experimental facility*. International Journal of Hydrogen Energy, 2009. **34**: p. 5902-5911.
- [15] Lacombe, J.M., Dagba, Y., Jamois, D., Perrette, L. and C.H. Proust, *Large scale hydrogen release in an isothermal confined area*. International Journal of Hydrogen Energy, 2011. **36**(3): p. 2302-2312.
- [16] Barley, C.D. and K. Gawlik, *Buoyancy-driven ventilation of hydrogen from buildings: laboratory test and model validation*. International Journal of Hydrogen Energy, 2009. **34**: p. 5592-5603.
- [17] Agarant, V., Cheng, Z. and A. Tchouvelev. *CFD modeling of hydrogen releases and dispersion in hydrogen energy station*. in *Proceedings of the fifteenth World Hydrogen Energy Conference*. 2004. Yokohama.
- [18] Matsuura, K., Kanayama, H., Tsukikawa, H. and M. Inoue, *Numerical simulation of leaking hydrogen dispersion behavior in a partially open space*. International Journal of Hydrogen Energy, 2008. **33**(1): p. 240-247.

- [19] K. Matsuura, *Effects of the geometrical configuration of a ventilation system on leaking hydrogen dispersion and accumulation*. International Journal of Hydrogen Energy, 2009. **34**(24): p. 9869-9878.
- [20] Matsuura, K., Nakano, M. and J. Ishimoto, *The sensing-based adaptive risk mitigation of leaking hydrogen in a partially open space*. International Journal of Hydrogen Energy, 2009. **34**(20): p. 8770-8782.
- [21] Makarov, D.V. and V.V. Molkov, *Modeling and Large Eddy Simulation of Deflagration Dynamics in a Closed Vessel*. Combustion, Explosion, and Shock Waves, 2004. **40**(2), p. 136-144.
- [22] Molkov, V. Makarov, D. and H. Schneider, *LES modelling of an unconfined large-scale hydrogen-air deflagration*. Journal of Physics D: Applied Physics, 2006. **39**: p. 4366-4376.
- [23] Chernyavsky, B., Wu, T.C., Péneau, F., Bénard, P., Oshkai, P. and N. Djilali *Numerical and experimental investigation of buoyant gas release: Application to hydrogen jets*. International Journal of Hydrogen Energy, 2011. **36**: 2645-2655.
- [24] Haley, A.A. and A. Banerjee *Role of initial conditions in unstably stratified hydrogen-air mixing zones*. International Journal of Hydrogen Energy, 2011. **36**: p. 11174-11182.
- [25] Sharma, P.K., Gera, B. and R.K. Singh, *Application of RANS and LES Based CFD to Predict the Short and Long Term Distribution and Mixing of Hydrogen in a Large Enclosure*. CFD Letters, 2011. **3**(1): p. 18-31.
- [26] Erlebacher, G., Hussaini, M.Y., Speziale, C.G. and T.A. Zang, *Toward the Large-Eddy Simulation of Compressible Turbulent Flows*. Journal of Fluid Mechanics, 1992. **238**: p. 155-185.
- [27] E.R. Van Driest, *On Turbulent Flow Near a Wall*. Journal of the Aeronautical Sciences, 1956. **23**(11): p. 1007-1011, 1036.
- [28] Venetsanos, A.G., Papanikolaou, E. and J.G. Bartzis, *The ADREA-HF CFD code for consequence assessment of hydrogen applications*. International Journal of Hydrogen Energy, 2010. **35**: p. 3908-3918.
- [29] Kovalets, I.V., Andronopoulos, S., Venetsanos, A.G. and J.G. Bartzis, *Optimization of the numerical algorithms of the ADREA-I mesoscale prognostic meteorological model for real-time applications*. Environmental Modelling & Software, 2008. **23**: p. 96-108.
- [30] Ferziger, J.H. and Perić M. Computational Methods for Fluid Dynamics. 3rd ed. Springer-Verlag. Berlin. 2002.
- [31] Saad, Y. Iterative methods for sparse linear systems. 2nd ed. SIAM. Philadelphia. 2003.
- [32] Papanikolaou, E.A., Venetsanos, A.G., Heitsch, M., Baraldi, D., Huser, A., Pujol, J., Garcia, J. and N. Markatos, *HySafe SBEP-V20: Numerical studies of release experiments inside a naturally ventilated residential garage*. International Journal of Hydrogen Energy, 2010. **35**(10): p. 4747-4757.
- [33] McGrattan, K., Hostikka, S., Floyd, J. and R. McDermott, *Fire Dynamics Simulator (Version 5), Technical Reference Guide. Volume 3: Validation*, National Institute of Standards and Technology, U.S. Department of Commerce. 2010. http://fds-smv.googlecode.com/svn/trunk/FDS/trunk/Manuals/All_PDF_Files/FDS_Validation_Guide.pdf (accessed 3-7-2012).
- [34] Zhang, J., Delichatsios, M.A. and A.G. Venetsanos, *Numerical studies of dispersion and flammable volume of hydrogen in enclosures*. International Journal of Hydrogen Energy, 2010. **35**: p. 6431-6437.
- [35] McGrattan, K., Hostikka, S., Floyd, J., Baum, H., Rehm, R., Mell, W. and R. McDermott, *Fire Dynamics Simulator (Version 5), Technical Reference Guide. Volume 1: Mathematical model*. National Institute of Standards and Technology, U.S. Department of Commerce. 2010. http://fds-smv.googlecode.com/svn/trunk/FDS/trunk/Manuals/All_PDF_Files/FDS_Technical_Reference_Guide.pdf (accessed 3-7-2012).